J|A|C|S

A R T I C L E S

New Nickel(II) Diimine Complexes and the Control of Polyethylene Microstructure by Catalyst Design

Dieter Meinhard,[†] Marcus Wegner,[†] Georgy Kipiani,[†] Andrew Hearley,[†] Peter Reuter,[†] Stefan Fischer,[‡] Othmar Marti,[‡] and Bernhard Rieger*,[§]

Contribution from the Institute of Inorganic Chemistry II, Ulm University, Albert-Einstein Allee 11, 89081 Ulm, Germany, Institute for Experimental Physics, Ulm University, Albert-Einstein-Allee 11, 89081 Ulm, Germany, and Wacker - Lehrstuhl für Markomolekulare Chemie, Technische Universität München, Lichtenbergstr. 4, 85747 Garching, Germany
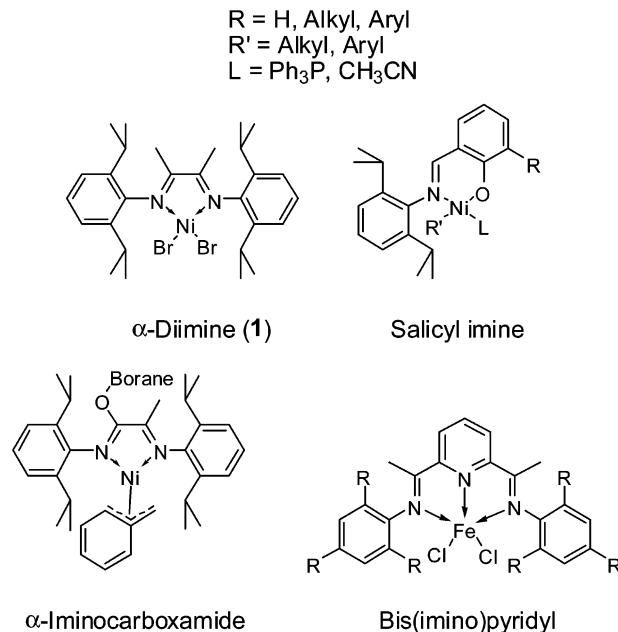
Received January 18, 2007; E-mail: rieger@tum.de

Abstract: Starting from differently substituted boronic acids as versatile building block, new "*ortho*-aryl" α-diimine ligands **a**−**h** were synthesized in an easy, high-yielding route. Reaction of the complex precursor diacetylacetonato-nickel(II) with a trityl salt, like [CPh₃] [B(C₆F₅)₄] or [CPh₃] [SbCl₆], in the presence of the diimine ligands afford the monocationic, square planar complexes **2a**−**g** in almost quantitative yields. Suitable crystals (**2d′,e,f,g**) were submitted for X-ray diffraction analysis. A geometry model was developed to describe the orientation of ligand fragments around the nickel(II) center that influence the polymer microstructure. At elevated reaction temperature and pressure, and in the presence of hydrogen, **2a**−**e** catalyze the homopolymerization of ethylene to give branched PE products ranging from HD- to LLD-PE grades. The polymerization results indicate the possibility of precise microstructure control depending on the particular complex substitution. Preliminary investigations on material density and mechanical behavior by uniaxial stretching until failure point toward new material properties that can result from the simple ethylene monomer by catalyst design.

1. Introduction

The application of late transition metal complexes like **1** (Chart 1) by Brookhart in the mid-1990s marked a breakthrough in homogeneous polymerization catalysis. In contrast to metallocene catalysts,[1] based on early transition metals, his Ni(II) and Pd(II) species produced branched polyethylene grades,[2] varying in concentration and individual length of branches, exclusively from the ethylene monomer and accommodated even

† Institute of Inorganic Chemistry II, Ulm University.
‡ Institute for Experimental Physics, Ulm University.
§ Technische Universität München.
(1) (a) Blom, R.; Follestad, A.; Rytter, E.; Tilset, M.; Ystenes, M.; *Organometallic Catalysts and Olefin Polymerization − Catalysts for a new Millennium*; Springer-Verlag: 2001. (b) Kaminsky, W., Sinn, H., Eds. *Olefin Polymerization*; Springer-Verlag: 1988. (c) Quirk, R. P., Ed. *Transition Metal Catalyzed Polymerizations Ziegler-Natta and Metathesis Polymerizations*; Cambridge University Press: 1988. (d) Moulijn, J. A., van Leeuwen, P. W. N. M., van Santen, R. A., Eds. *Catalysis − An integrated Approach to Homogeneous, Heterogeneous and Industrial Catalysis*; Elsevier: Amsterdam, 1993. (e) Fink, G.; Mühlhaupt, R., Brintzinger, H. H., Eds. *Ziegler Catalysts*; Springer-Verlag: 1995. (f) Scheris, J., Kamisky, W., Eds. *Metallocene-Based Polyolefins: Preparation, Properties and Technology*; John Wiley & Sons Ltd.: 2000. (g) A fine series of reviewing articles: Alt, H. G.; Köppl, A. *Chem. Rev.* **2000**, *100* (4), 1205. Coates, G. W. *Chem. Rev.* **2000**, *100* (4), 1223. Resconi, L.;Cavallo, L.; Fait, A.; Piemontesi, F. *Chem. Rev.* **2000**, *100* (4), 1253. Hlatky, G. G. *Chem. Rev.* **2000**, *100* (4), 1347. Fink, G.; Steinmetz, B.; Zechlin, J.; Przybyla, C.; Tesche, B. *Chem. Rev.* **2000**, *100* (4), 1377. Chen, E. Y-X.; Marks, T. J. *Chem. Rev.* **2000**, *100* (4), 1391. Rappé, A. K.; Skiff, W. M.; Casewit, C. J. *Chem. Rev.* **2000**, *100* (4), 1435. Angermund, K.; Fink, G.; Jensen, V. R.; Kleinschmidt, R. *Chem. Rev.* **2000**, *100* (4), 1457. Baird, M. C. *Chem. Rev.* **2000**, *100* (4), 1471. Boffa, L. S., Novak, B. M. *Chem. Rev.* **2000**, *100* (4), 1479. (h) Brintzinger, H. H.; Fischer, D.; Mülhaupt, R.; Rieger, B.; Waymouth, R. *Angew. Chem., Int. Ed. Engl.* **1995**, *34* (11), 1143.
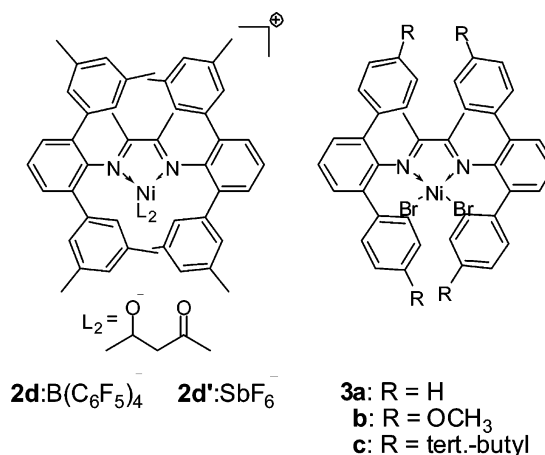
Chart 1. Important Late Transition Metal Complexes

α-Diimine (**1**)   Salicyl imine

α-Iminocarboxamide   Bis(imino)pyridyl

polar monomers, like acrylates.[3] These findings triggered the development of a series of new complexes. Among the most significant results in this field are highly active and versatile catalysts based on bidentate diimine [N,N],[2] salicyl imine [N,O],[4] or iminocarboxamide [N,N/O][5] palladium and nickel

complexes and tridentate 2,6-bis(imino)-pyridyl [N,N,N] iron and cobalt[6] complexes (Chart 1). Even the production of aqueous polyethylene dispersions using catalysts of the salicyl imine type has become possible.[7]

The alkyl side chains introduced to the polymer backbone through a "chain walking" mechanism by the 1,4-diazabutadiene catalyst **1**, however, lead for the first time to LLDPE made exclusively from ethylene.[8] This discovery caused considerable interest, since it allows us to generate high value branched polymers without the application of expensive 1-alkene comonomers (e.g., 1-butene, 1-hexene, 1-octene, or longer).[9] However, one major drawback for commercialization is the rapid and quantitative deactivation of catalytically active Ni(II) species in the presence of hydrogen, which is inevitable for molecular weight control in technical polymerization processes.[10]

Recently, we reported on a new "*ortho*-aryl effect" using terphenyl substituted 1,4-diaza-1,3-butadiene ligands.[11] The corresponding nickel(II) complexes (e.g., **3a**−**c**, Chart 2) are excellent, highly active catalysts for ethylene homopolymerization reactions that produce almost perfectly linear polyethylenes in the presence of hydrogen. The present contribution reports on 3,5-substituted terphenyl α-diimine ligands and their corresponding monocationic Ni(II) complexes (Chart 3, **2a**−**g**). The "*ortho*-aryl" groups are prone to easy chemical modification and are therefore ideal candidates for a micro-

Chart 2. Polyaromatic α-Diimine Nickel(II) Complex Family

2d:B(C₆F₅)₄   **2d'**:SbF₆   **3a**: R = H
                                  b: R = OCH₃
                                  c: R = tert.-butyl

structure control of LLDPE products by catalyst design.[11,12] Material properties of selected LLDPE grades prepared by **2b,d**/TMA are discussed.

2. Results and Discussion

2.1. Synthesis and Characterization of the α-Diimine Ni(II) Complexes. Starting from differently substituted phenyl boronic acids and 2,6-dibromoaniline, the corresponding 2,6-diphenyl-anilines were prepared by Suzuki cross coupling reactions (Scheme 1).[11,13,14] Acid-catalyzed condensation with α,β-diketones, like 2,3-butadione or acenaphthenequinone, affords **a**−**h** in up to 80% yield.[15] Reaction of NiBr₂ precursors, like (DME)NiBr₂, with an α-diimine ligand of lower steric demand, e.g., *N,N'*-bis-2,6-diisopropylphenyl-1,4-diaza-2,3-dimethyl-1,3-butadiene, leads to the corresponding complex **1**, as expected.[2] However, all attempts to produce crystallizable neutral NiCl₂ or NiBr₂ complexes derived from the aryl substituted α-diimine ligands **a**−**h** failed.

A strategy for an efficient synthesis of such bulky complexes uses trityl tetrakis(pentafluorophenyl)borate ([Ph₃C][B(C₆F₅)₄]) or trityl hexachloroantimonate ([Ph₃C][SbCl₆]), which abstracts one acetylacetonato (acac) ligand from the Ni(acac)₂ precursor in the presence of **a**−**g**. This convenient route gives the crystalline, monocationic complexes **2a**−**g** in up to 95% isolated yields (Chart 3).[16,17]

We obtained single crystals suitable for X-ray diffraction analysis by slow diffusion of *n*-pentane in a dichloromethane solution of **2d′**, **e**, **f**,[18] and **g** (Figures 1 and 2). The unit cell includes two (**2d′,e**) or four (**2f,g**) ion pairs, respectively. In contrast to the tetrahedral dibromo complexes of type **1**, the

(2) (a) Brookhart, M.; Johnson, L. K.; Killian, C. M. *J. Am. Chem. Soc.* **1995**, *117*, 6414. (b) Rieger, B.; Baugh, L. S.; Kacker, S.; Striegler, S., Eds. *Late Transition Metal Polymerization Catalysis*; Wiley - VCH: Weinheim, Germany, 2003; p 331. (c) Brookhart, M.; Ittel, S. D.; Johnson, L. K. *Chem. Rev.* **2000**, *100*, 1169. (d) Gibson, V. C.; Spitzmesser, S. K. *Chem. Rev.* **2003**, *103*, 283. (e) Gates, D. P.; Svejda, S. A.; Onate, E.; Killian, C. M.; Johnson, L. K.; White, P. S.; Brookhart, M. *Macromolecules* **2000**, *33*, 2320.

(3) (a) Johnson, L. K.; Mecking, S.; Brookhart, M. *J. Am. Chem. Soc.* **1996**, *118*, 267. (b) Mecking, S.; Johnson, L. K.; Wang, L.; Brookhart, M. *J. Am. Chem. Soc.* **1998**, *120*, 888. (c) Heinemann, J.; Mülhaupt, R.; Brinkmann, P.; Luinstra, G. *Macromol. Chem. Phys.* **1999**, *200* (2), 384. (d) Michalak, A.; Ziegler, T. *J. Am. Chem. Soc.* **2001**, *123* (49), 12266. (e) Philipp, D. M.; Muller, R. P.; Goddard, I., W. A.; Storer, J.; McAdon, M.; Mullins, M. *J. Am. Chem. Soc.* **2002**, *124* (34), 10198. (f) Gottfried, A. C.; Brookhart, M. *Macromolecules* **2001**, *34* (5), 1140. (g) Popeney, C.; Guan, Z. *Organometallics* **2005**, *24* (6), 1145.

(4) (a) Wang, C.; Friedrich, S.; Younkin, T. R.; Li, R. T.; Grubbs, R. H.; Bansleben, D. A.; Micheal, W. D. *Organometallics* **1998**, *17* (15), 3149. (b) Younkin, T. R.; Connor, E. F.; Henderson, J. I.; Friedrich, S. K.; Grubbs, R. H.; Bansleben, D. A. *Science* **2000**, *287*, 460. (c) Goettker-Schnetmann, I.; Wehrmann, P.; Roehr, C.; Mecking, S. *Organometallics* **2007**, *26* (9), 2348.

(5) (a) Lee, B. Y.; Bazan, G. C.; Vela, J.; Komon, Z. J. A.; Bu, X. *J. Am. Chem. Soc.* **2001**, *123* (22), 5352. (b) Diamanti, S. J.; Ghosh, P.; Shimizu, F.; Bazan, G. C. *Macromolecules* **2003**, *36* (26), 9731.

(6) (a) Brookhart, M.; Small, B. L.; Bennett, A. M. A. *J. Am. Chem. Soc.* **1998**, *120*, 4049. (b) Britovsek, G. J. P.; Gibson, V. C.; Kimberley, B. S.; Maddox, P. J.; McTavish, S. J.; Solan, G. A.; White, A. J. P.; Williams, D. J. *Chem. Commun.* **1998**, 849. (c) Britovsek, G. J. P.; Bruce, M.; Gibson, V. C.; Kimberley, B. S.; Maddox, P. J.; Mastroianni, S.; McTavish, S. J.; Redshaw, C.; Solan, G. A.; Strömberg, S.; White, A. J. P.; Williams, D. J. *J. Am. Chem. Soc.* **1999**, *121*, 8728.

(7) (a) Held, A.; Bauers, F. M.; Mecking, S. *Chem. Commun.* **2000**, *4*, 301. (b) Zuideveld, M. A.; Wehrmann, P.; Röhr, C.; Mecking, S. *Angew. Chem.* **2004**, *116*, 887 or *Angew. Chem., Int. Ed.*, **2004**, *43* (7), 869.

(8) Guan, Z.; Cotts, P. M.; McCord, E. F.; McLain, S. J. *Science* **1999**, *238*, 2059.

(9) In the year 2004 35 Mio tons of PE-LD/PE-LLD and 25 Mio tons of PE-HD were consumed worldwide, and consumption is considered to grow by 5% p.a. at least until 2010. PlasticsEurope Deutschland, WG Statistics and Market Research; cf. *http://www.vke.de/de/infomaterial/download/*.

(10) (a) The genuine reason, however, for this unexpected reactivity difference still remains unclear. We are making investigations on this interesting effect and will publish the first results soon. (b) For technical reasons heterogeneous catalysts are mainly used in industry. (c) A fine study with a related acenaphthene backbone α-diimine dibromo nickel(II) complex to its polymerization behaviour in the presence of hydrogen was published earlier, proving the rapid and quantitative deactivation of the complex. cf. de Souza, R. F.; Mauler, R. S.; Rochefort Neto, O. I. *Macromol. Chem. Phys.* **2001**, *202* (17), 3432.

(11) Schmid, M.; Eberhardt, R.; Klinga, M.; Leskelä, M.; Rieger, B. *Organometallics* **2001**, *20* (11), 2321.

(12) (a) Ionkin, A. S.; Marshall, W. J. *J. Organomet. Chem.* **2004**, *689* (6), 1057. (b) Ionkin, A. S.; Marshall, W. J. *Organometallics* **2004**, *23* (13), 3276.

(13) Miura, Y.; Oka, H.; Momoki, M. *Synthesis* **1995**, *1995* (11), 1419.

(14) Kipiani, G. Ph.D. Thesis, University Ulm, 2005.

(15) The yields depend strongly on the individual substitution pattern. Introducing sterically demanding groups R¹−R³ to the aniline fragments or R′ of the α,β-diketones leads to a decline in yield.

(16) Moody, L. S.; Mackenzie, P. B.; Killian, C. M.; Lavoie, G. G.; Ponasik, J. A., Jr.; Barrett, A. G.; Smith, T. W.; Pearson, J. C. WO 00/50470, 2000.

(17) For a nice synthesis strategy towards the analogue η³-allyl *N,N'*-bis(2,6-bis(3-trimethylsilylphenyl)phenyl)-1,4-diaza-2,3-dimethyl-1,3-butadiene nickel-(II) complex, cf.: Ionkin, A. S.; Marshall, W. J. *J. Organomet. Chem.* **2004**, *689* (6), 1057.

(18) Experiments that afford single crystals of **2a** suitable for X-ray diffraction analysis were not successful. Therefore, we applied the relative system **2g** with two methyl substituents in para-position to the aza-group. We suggest that these methyl groups, at the periphery of the complex structure, have a negligible steric effect on its solid state geometry.

Chart 3. α-Diimine Nickel(II) Complexes Used for Polymerization Reactions
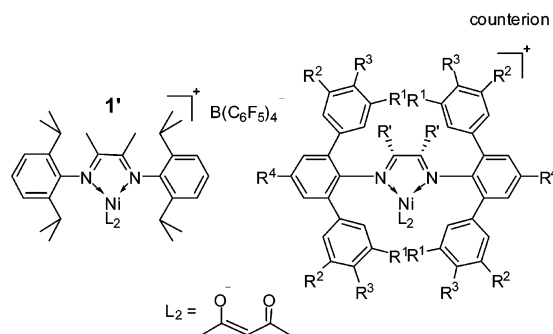
Compound number	R^1	R^2	R^3	R^4	R'	Counter ion
2a	H	H	H	H	CH_3	$B(C_6F_5)_4^-$
2b	CH_3	H	H	H	CH_3	$B(C_6F_5)_4^-$
2c	CF_3	H	H	H	CH_3	$B(C_6F_5)_4^-$
2d	CH_3	CH_3	H	H	CH_3	$B(C_6F_5)_4^-$
2d'	CH_3	CH_3	H	H	CH_3	SbF_6^-
2e	F	F	H	H	CH_3	$B(C_6F_5)_4^-$
2f	H	H	$C(CH_3)_3$	H	CH_3	$B(C_6F_5)_4^-$
2g	H	H	H	CH_3	CH_3	$B(C_6F_5)_4^-$
2h	CH_3	CH_3	H	H	Acenaphthen	$B(C_6F_5)_4^-$

nickel centers of the monocationic acac-complex **2d'–g** are located in a square planar ligand coordination sphere defined by N1, N2, O1, and O2. **2d'–g** are highly soluble in organic solvents and NMR investigations are possible, due to their exclusive diamagnetic character. The fact that **2a–g** can be investigated by NMR techniques suggests a similar coordination geometry in all of these compounds. The terphenyl moieties of **2d'–g** are large enough so that there is free rotation around the C–N imine single bonds; additionally, those around the C–C diaryl bonds are suppressed.[2,11]

The results of the X-ray structure analysis of **2d'–g** show that substituents (R^1–R^3, Chart 3) have a significant influence on coordination geometry. The unsubstituted phenyl rings in the 2,6-position of the aniline fragments in **2g** point toward each other above and below the plane, thus shielding the apical positions of the Ni(II) center. This affords an almost ideal C_{2v}-symmetry in **2g**. One may suggest that introducing groups in the 3,5-position leads to a disturbance of the geometry caused by repulsive interactions between substituents. However, 3,5-substituted aniline fragments (**2d',e**) obviously lock the phenyl moieties effectively into their face-to-face configuration. Substitution in the 4-position by bulky *tert*-butyl groups (**2f**) leads to a racemic mixture of complexes that adopt a chiral C_2-symmetric coordination geometry.

To give a more quantitative description of the substituent influence on complex structure, angles α, β, γ, and δ were introduced. The phenyl planes, the centroids, and the derivative plane vectors were calculated by least-squares methods, using the corresponding X-ray diffraction data. The apex angle α is determined by the vectors $\vec{E}_\alpha 1$ and $\vec{E}_\alpha 2$, building the connection line between the centroids of the three phenyl moieties on each
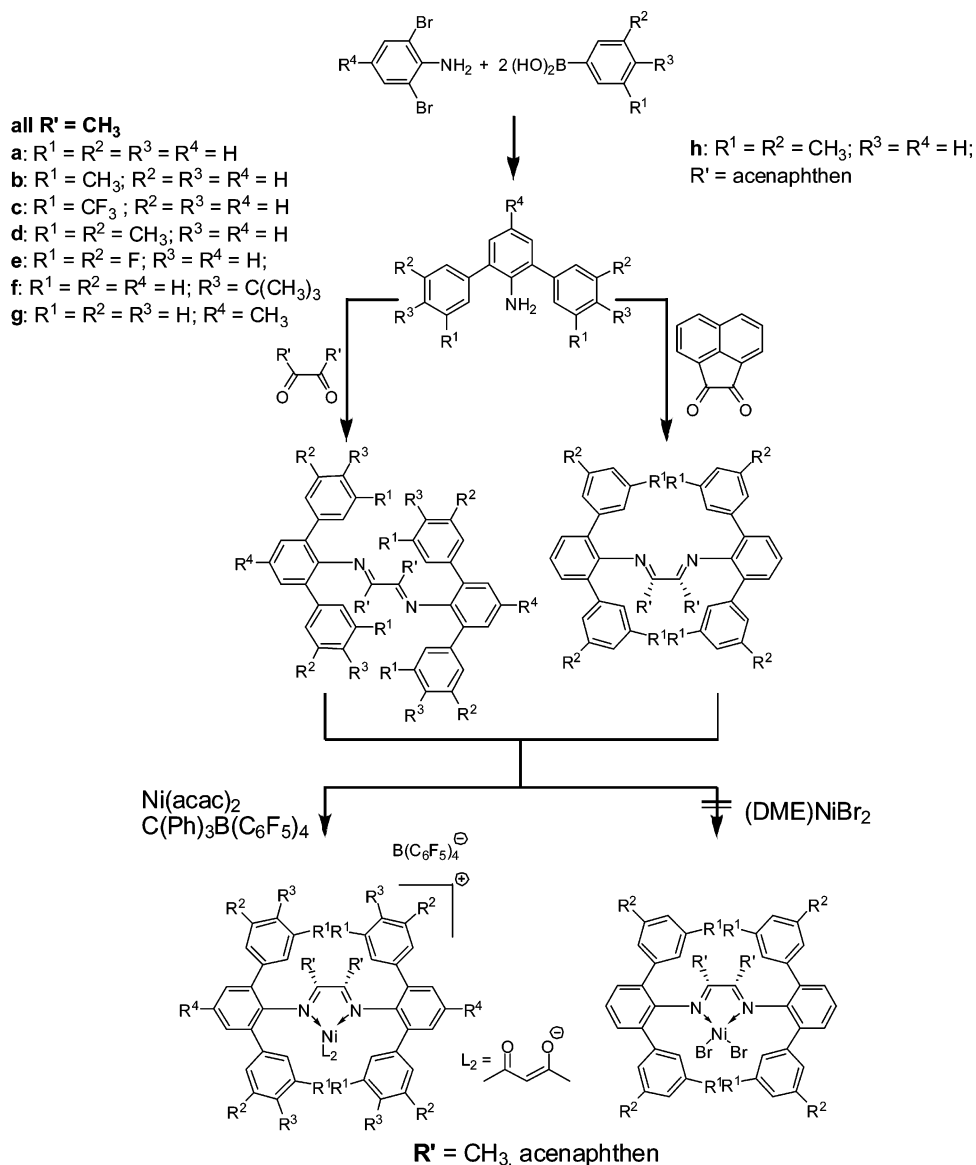
terphenyl wing (Scheme 2). β is a measure of the staggered arrangement within the terphenyl substituents and is given as the angle between the plane vectors $\vec{E}_\beta 1$ and $\vec{E}_\beta 2$. γ describes the level of distortion of the terphenyl wings and is given as the angle between plane vectors $\vec{E}_\gamma 1$ and $\vec{E}_\gamma 2$. Altogether they define the conelike space in front of the catalytically active nickel(II) center, which is assumed to have a major influence on the rate of ethylene coordination relative to the rate of chain walking, thus defining the length and concentration of the branches. δ shows the distortion of the square planar ligand sphere surrounding the nickel center, determined by the torsion angle between the CN double bond ($\vec{E}_\delta 1$) and the NiO bond ($\vec{E}_\delta 2$).

The ecliptic conformation of **2d'** and **2e** (γ = 6.4° and 13.4°, respectively) indicates that there is almost no distortion induced by the 3,5-substitution, opening space for isomerization (chain walking) reactions in the front of the catalytically active nickel center. γ increases to 24.74° for **2g** in the absence of a sterically demanding substituent. Therefore, we suggest that the deviation from ideal C_{2v}-symmetry is a superior effect of nonbond contacts between the terphenyl moieties and the diacetyl backbone or the acetylacetonato rest and resembles a kind of a "frozen conformation" in the solid state.[19] However, γ is increased to 65.9° in **2f** and the structure is finally altered into the chiral C_2-symmetry with the smallest cone volume, reducing the probability for chain walking (formation of bulky olefin complexes by β-H-elimination), so that nearly linear polyethylene is formed. The 4-*tert*-butyl phenyl substituents pointing toward the nickel(II) center force the two oxygen atoms of the acac ligand to give up the favored positions in a square planar coordination geometry of the nickel, affording δ = 10.1°. However, we could not detect any signal broadening in the ^{1}H NMR experiment that may result from changes in the magnetic character. The same sterical as well as NMR effects are observed for the rear dimethyl substituents of the ligand backbone.

Interestingly, although **2f** has a 4-*tert*-butyl substitution, the values for α are similar for **2e, f**, and **g** (125.0°, 124.4°, and 129.6°, respectively). **2f** avoids this sterical stress by γ-distortion corresponding to rotation around the C–N bond of the aniline fragment and by the staggered conformation of its 2,6-phenyl substituents (β = 79.4°, corresponding to a rotation around the aryl–aryl bond). The 3,5-dimethyl substituted **2d'**, however, has a structure of α = 133.7°, which offers the largest cone volume for ethylene insertions and chain-walking processes.

2.2. Polymerization Experiments. Polymerization activity and product properties are determined by a wide range of process parameters. We mainly focus on investigating reaction temperature, monomer pressure, hydrogen concentration, and especially the influence of the ligand architecture. Preliminary ethylene polymerization reactions were performed, using the complex **2d** to study different activators and to find the optimal Al/Ni ratio. Therefore, catalytically active species were generated *in situ* by reaction of **2d** with TMA, MAO, or triisobutylaluminum (TiBA), respectively. Clearly, the highest activity was achieved with the TMA activator (Table 1, Figure 3). Since the activation mechanism obviously affords exchange of the

(19) In an attempt to give a quantification of the expression "frozen conformation", we calculated the unusually short nonbond contacts in **2g** (sum of the particular van der Waals radii, 0.1 Å) and found exclusively intramolecular contacts fitting this particular coordination geometry. (The values are tabulated in the Supporting Information).

Scheme 1. Synthesis of Monocationic α-Diimine Nickel(II) Complexes Starting from Differently Substituted Boronic Acids

all R' = CH₃
a: $R^1 = R^2 = R^3 = R^4 = H$
b: $R^1 = CH_3$; $R^2 = R^3 = R^4 = H$
c: $R^1 = CF_3$; $R^2 = R^3 = R^4 = H$
d: $R^1 = R^2 = CH_3$; $R^3 = R^4 = H$
e: $R^1 = R^2 = F$; $R^3 = R^4 = H$;
f: $R^1 = R^2 = R^4 = H$; $R^3 = C(CH_3)_3$
g: $R^1 = R^2 = R^3 = H$; $R^4 = CH_3$

h: $R^1 = R^2 = CH_3$; $R^3 = R^4 = H$;
R' = acenaphthen

R' = CH₃, acenaphthen

remaining acetylacetonato ligand by an Al(III)−alkyl group, the least sterically demanding aluminum compound was expected to most efficiently activate the Ni(II) centers. MAO gives at the same Al/Ni ratio (Al/Ni = 500) only about 25% of the TMA activity. It is not clear if this is a result of the steric demand of the oligomeric MAO molecules or of the low TMA content which is always present in MAO solutions. The hypothesis that steric considerations play a major role in activation of such "*ortho*-aryl" acac complexes is supported by experiments applying TiBA, which hardly shows any polymerization activity.

In addition, the particular ratio of aluminum to nickel plays an important role for catalyst activity (Figure 3). Below a threshold of Al/Ni = 200, no activation reaction can be observed (Table 1, entry 1). The genuine reason for that effect still remains unclear. However, low aluminum concentrations ([Ni]$_{const}$ = 10 μmol/ 800 mL) might, even at constant Al/Ni ratios, hinder efficient activation, due to slow alkylation reactions or to Al−alkyl scavenging effects.[20] The highest activities were found at a TMA/Ni ratio of 500. Increasing the Al(III) concentration, exceeding an Al to Ni ratio of 500, facilitates most probably

dialkylation of the nickel centers. Such nickel−dialkyl intermediates deactivate rapidly and quantitatively by reductive elimination to nickel(0).[21] Another potential explanation is deactivation by reaction of the imine ligand fragments with TMA.[22]

It is important to note that the different activators as well as the nickel to aluminum ratio show no influence on the product properties, like T_m and molecular weight (Table 1). Thus, all further investigations were performed using TMA at Al/Ni = 500.

Catalytically active species derived from the monocationic "diisopropyl" complex **1** or from neutral **1′** by reaction with TMA deactivate rapidly and quantitatively in the presence of hydrogen. At ambient temperature, we could not detect any activity when hydrogen was applied to control molecular weight (Table 2, entry 9). At 60 °C, the ethylene flow curve of **1′**/TMA indicates a regular starting activity, followed by a rapid

(20) Toluene was distilled of LiAlH₄ prior to use. See the Experimental Section in the Supporting Information.
(21) Svoboda, M.; tom Dieck, H. *J. Organomet. Chem.* **1980**, *191*, 321.
(22) Cámpora, J.; del Mar Conejo, M.; Mereiter, K.; Palma, P.; Pérez, C.; Reyes, M. L.; Ruiz, C. *J. Organomet. Chem.* **2003**, *683*, 220.
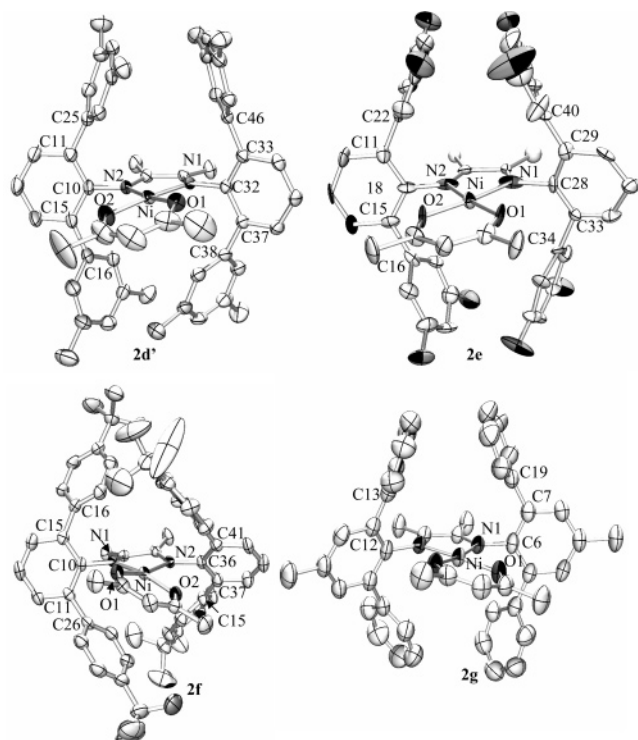
Figure 1. Pov-Ray imaged ORTEP plots of **2d′**, **2e**, **2f**, and **2g** labeled with important atoms (front view). The atoms are drawn as 50% thermal ellipsoids. Solvent molecules, hydrogen atoms, and the particular counterion are omitted for clarity.

descent instead of a low level polymerization reaction over the entire experiment (Figure 4). In contrast, all the aryl-substituted species **2a–e**/TMA polymerize ethylene in the presence of hydrogen on a continuously high level. At ambient temperature, **2a**/TMA shows an exceptionally high activity that even exceeds the measuring scale of the particular flow meter applied during the initial phase.

An activity decline with growing sterical demand of the ligand was observed as a general trend (Figure 5) by introducing four (**2b,c**) or eight (**2d,e**) *meta* substituents on the "*ortho*-aryl" rings.[23] At 60 °C, the "unsubstituted" **2a**/TMA gives the highest activity, followed closely by **2b**/TMA. Interestingly, exchange of the four CH$_3$ substituents with four CF$_3$ groups (**2b** → **2c**)[24] affords a significant activity reduction by a factor of about 8. The lowest activities are therefore identified in the case of the catalysts **2d**/TMA and **2e**/TMA, as expected. The same behavior was found at T_p = 80 °C under comparable experimental conditions (Figure 6).

To our surprise, the trend for molecular weight did not follow the sterical demand of the ligand substitution. We were expecting an M_w decrease in the series **2a** > **2b** ≈ **2c** > **2d** ≈ **2e**, due to a higher isomerization rate slowing down chain
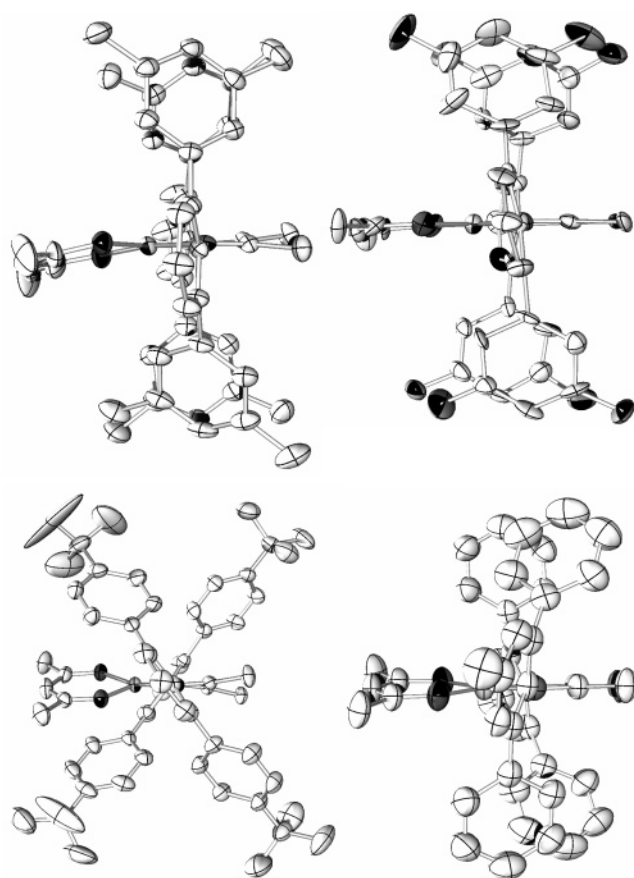
(23) Due to highly differing catalyst activities at ambient temperature we were forced to run polymerization experiments in a wide time range of 2 min up to 1 h. It appeared that dilution of the nickel complex was no solution of this challenge, since this did not lead to a linear decrease of activity. In addition, besides precipitation of polymer product or changes in viscosity of the polymer solutions, all detailed discussions of catalyst activities are problematic at this stage because the contribution of ligand substitution to a "catalyst intrinsic" activity relative to the question of the fraction of activated Ni(II) centers remains open.

(24) A study on a fluorine effect on polyphenyl substituted α-diimine complexes was published earlier; cf. ref 2b. Moreover, for a series of fine papers on a fluorine effect in water soluble Grubbs-type catalysts for a polyethylene emulsion polymerization reaction, cf. ref 7b.

Figure 2. Pov-Ray imaged ORTEP plots of **2d′**, **2e**, **2f**, and **2g** (side view). The atoms are drawn as 50% thermal ellipsoids. Solvent molecule, hydrogen atoms, and the particular counterion are omitted for clarity.

propagation. Catalysts **2c, e**, however, bearing fluorine substituents, are producing a notably higher molecular weight M_w compared to their alkyl substituted analogues (Figure 7). We have no genuine explanation for this effect. We suggest that an interaction between the fluorine atoms and Al(III) activators blocks the apical positions of the catalytically active nickel center, which may reduce effectively associative olefin exchange reactions.[25]

The application of hydrogen makes molecular weight tunable, e.g., 5 × 10^5 to 1 × 10^5 g/mol with **2d**/TMA or 9 × 10^5 to 3 × 10^5 g/mol with **2e**/TMA, without a significant change in polymerization activity at 60 °C. The molecular weight distribution of the polyethylene grades lies in the typical range for single site catalysts.[2b]

The formation of alkyl branches on the polyethylene main chain results from a three-step reaction sequence allowing the polymerization active metal complex to move along the chain ("chain walking") between two consecutive ethylene insertions ("chain propagation"). β-Hydride elimination initially forms a nickel hydride species, coordinated weakly by a vinyl end-capped polymer chain.[26] Rotation around this Ni–alkene π-bond

(25) To support the hypothesis that electronic effects play a minor role on the polymerization performance, especially referring to M_w as well as the branching degree, we synthesized some polyaromatic α-diimine Ni(II) complexes bearing electronically withdrawing or donating groups (nitro and fluoro) *para* to the two imine functions. The aryl rings in the 2,6-position bear no substituents, like the parent structure **2a**. Comparing molecular weight and the polymer microstructure these complexes show similar results relative to the parent catalyst **2a**/TMA. We report in detail on the results in the Supporting Information.

Scheme 2. Definition of Angles for a Detailed Coordination Geometry Discussion
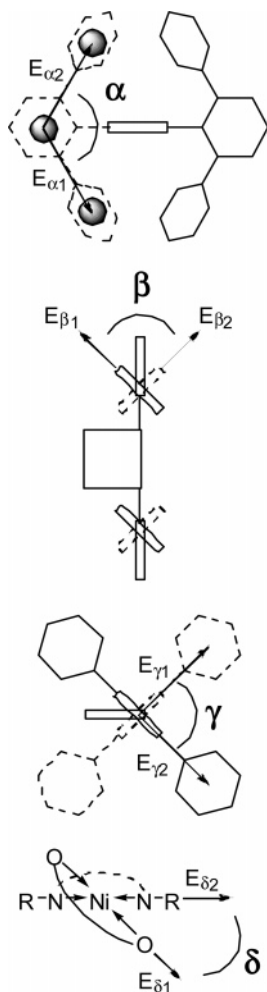
**Table 1.** Polymerization Parameter Search Results with **2d**

no.	activator[a]	H$_2$ time[b] [h]	vol[c] [mL]	Ni/Al ratio	yield [g]	activity [kg$_{Pol}$/ (g$_{Ni}$×h)]	M_w×10^{-5} [g/mol]	PDI	branching [‰]	mp [°C]
1	TMA	0.50	150	100	0	0	n.a.	n.a.	n.a.	n.a.
2	TMA	0.50	150	200	6.70	23	6.3	2.3	29	101.6
3	TMA	0.07	375	400	17.47	446	4.7	2.6	33	100.4
4	TMA	0.07	375	500	29.80	762	7.3	3.3	31	106.8
5	TMA	0.23	150	800	17.92	131	8.1	2.3	29	101.4
6	TMA	0.25	150	1600	11.50	78	7.5	2.0	29	101.6
7	MAO	0.08	375	500	9.98	204	8.5	3.1	28	108.0
8	TiBA	0.17	375	500	3.97	41	14.7	4.0	30	104.3

[a] General polymerization conditions 10 μmol cat., solvent toluene (800 mL), reaction temperature 80 °C and 30 bar ethylene pressure. [b] Due to high activity polymerizations were run shorter. [c] Preset amounts of hydrogen

and 2,1-reinsertion into the Ni−H fragment afford the first methyl branch ("chain end isomerization") on the polymer backbone.[8] Two major consequences result from this mechanistic scheme: the occurrence of branches reduces the polymerization activity and a statistically favored formation of methyl side groups.

At ambient temperature (30 °C, Table 2), the degree of branching is nearly independent from the particular ligand

(26) To suppress chain termination reactions the apical positions on the nickel catalyst have to be shielded. This important feature in α-diimine nickel complex chemistry was published earlier; cf. ref 2; Markus Schmid, Ph.D. Thesis, University Ulm, 1999.
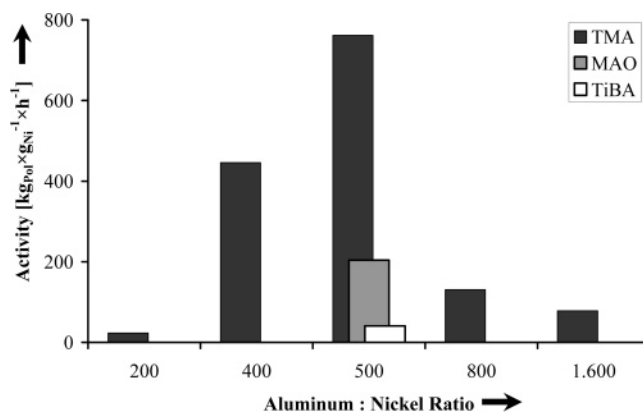
Figure 3. Comparison of the activators for **2d** and the Al/Ni ratios.

substitution of **2a−e** as well as from the reaction time. For example, **2d** bearing eight sterically demanding methyl groups and **2a** showing no phenyl substitution produce predominantly linear polyethylenes (Table 2 entries 17, 27). This indicates that propagation is privileged compared to chain walking (and therefore branching) under these conditions, as previously reported for other catalyst structures.[27,2,11b]

Due to its low exothermic character and a significantly higher activation barrier, this process, however, is favored compared to propagation at increased temperature. At 60 °C (Table 2) and especially at the technically more important polymerization temperature of 80 °C (Table 3), differences in the particular ligand structure (Figure 8) become dominant for the introduction of embranchments into the polymer main chain. For example, the "unsubstituted" catalyst **2a**/TMA still produces almost linear polymers (branching numbers ≈ 3‰)[28] leading to products melting around 130 °C (Figure 9). **2b,c**/TMA (four CH$_3$, CF$_3$ groups, respectively) produces polymers with approximately 15−30‰ embranchments, predominantly methyl groups, as expected.

Interestingly, also other branches up to hexyl groups can be clearly detected in the ^{13}C NMR and DEPT experiments (Figure 10). The intensive CH$_3$ peak at 14.1 ppm is typical for butyl and longer branches. The existence of longer side chains finds further support by the absence of a signal at 23.4 ppm, which is significant for butyl side chains, indicating the relatively low concentration of butyl groups alone. Furthermore, the "positive" chemical shifts (DEPT experiment) of secondary carbon atoms at 22.89, 29.57, and 32.15 ppm are characteristic for a α, γ, β-carbon sequence (Table 4, entry 13) of CH$_2$ groups in these positions on hexyl or longer branches.[29] Additionally, we detect

(27) Ziegler, T.; Deng, L.; Woo, T. K.; Cavallo, L.; Margl, P. M. *J. Am. Chem Soc.* **1997**, *119*, 6177.

(28) The degree of branching *B* can be estimated from the integrals (*I*) of the methylene, methin, and methyl groups in ^{1}H NMR experiments of the particular polyethylene: cf. ref 2. It is given in per 1000 carbon atoms (‰) of the polymer backbone (Tables 2 and 3). The standard proton NMR spectra were obtained from 5 wt % polymer in bromobenzene[d5] on a 500 MHz Bruker spectrometer. The spectra were zero-filled up to 64k points. Baseline correction was applied to the NMR spectra before integration.

$$B = \frac{\frac{1}{3}I_{CH_3}}{\frac{\left(I_{CH_2} - \left(\frac{1}{3}I_{CH_3}\right)\right)}{2} + \frac{1}{3}I_{CH_3}} \times 1000$$

(29) Galland, B. G.; da Silva, L. P.; Dias, M. L.; Crossetti, G. L.; Ziglio, C. M.; Filgueiras, C. M. *J. Polym. Sci., Part A: Polym. Chem.* **2004**, *42*, 2171.
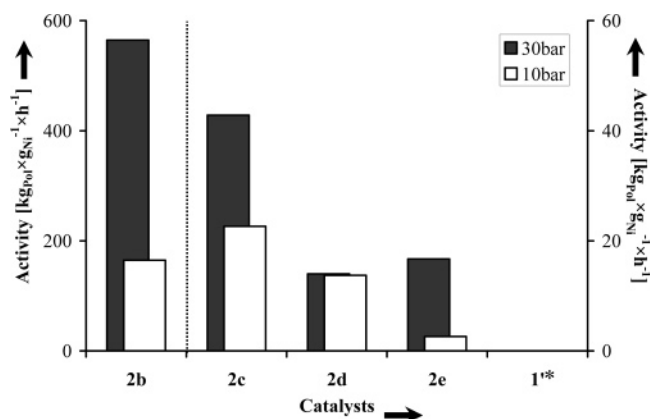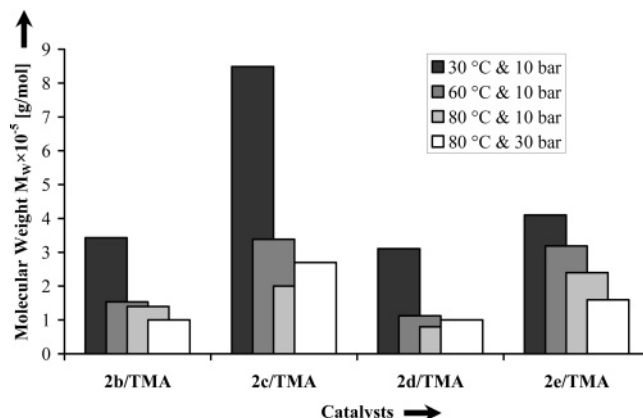
Table 2. Polymerization Results at 30 and 60 °C

no.	cat.[a]	time [h]	P [bar]	temp [°C]	X [m mmol H$_2$/ n mol C$_2$H$_4$]	activity [kg$_{Pol}$/ (g$_{Ni}$ × h)]	$M_W \times 10^{-5}$ [g/mol]	PDI	branches [‰]	T_m [°C]
9	1′	1.00	10	30	3.84	0	n.a.	n.a.	n.a.	n.a.
10	1′	0.17	10	60	0	135	4.6	2.5	83	37.1
11	1′	0.17	10	60	0.51	154	4.9	2.6	84	37.6
12	1′	0.17	10	60	3.84	27	3.2	2.3	85	39.2
13	2b	1.00	10	30	3.84	63	3.4	3.4	8	130.7
14	2b	0.17	10	60	3.84	369	1.5	2.2	11	129.0
15	2c	0.33	10	30	3.84	51	8.5	3.8	5	132.8
16	2c	0.17	10	60	3.84	100	3.4	2.1	24	113.8
17	2d	1.00	10	30	0	71	30.2	2.5	5	127.8
18	2d	1.00	10	30	3.84	68	3.1	2.4	6	128.9
19	2d	1.00	10	60	0	67	5.1	1.8	21	109.1
20	2d	1.00	10	60	0.51	60	3.4	2.3	29	102.4
21	2d	1.00	10	60	3.84	64	1.0	2.2	26	102.1
22	2d	0.33	30	60	3.84	372	1.1	2.2	23	110.1
23	2e	0.17	10	30	3.84	232	4.1	2.2	9	127.4
24	2e	0.17	10	60	0	97	9.0	2.4	33	101.4
25	2e	0.17	10	60	0.51	30	3.9	2.4	35	98.6
26	2e	0.17	10	60	3.84	136	3.2	2.3	32	100.4
27	2a	0.05	10	30	12.80	8414[b]	2.2	3.9	3	134.4
28	2a	0.05	10	60	12.80	408	3.1	3.5	3	128.6

[a] 800 mL of toluene, 10 μmol of **1**′, **2b−e** (in 4 mL of CH$_2$Cl$_2$) and 5 μmol (27) and 2.5 μmol (28) of **2a** (each in 4 mL of CH$_2$Cl$_2$); **1**′ and **2a−e** Al/Ni = 500. [b] The exact activity is hard to determine. We observed a rapid and uncontrolled temperature increase up to 45 °C in the initial 2 min, although we cooled the reaction matrix with 100% of available capacity. So we stopped the experiment after an additional minute to get 62 g of polymeric material.
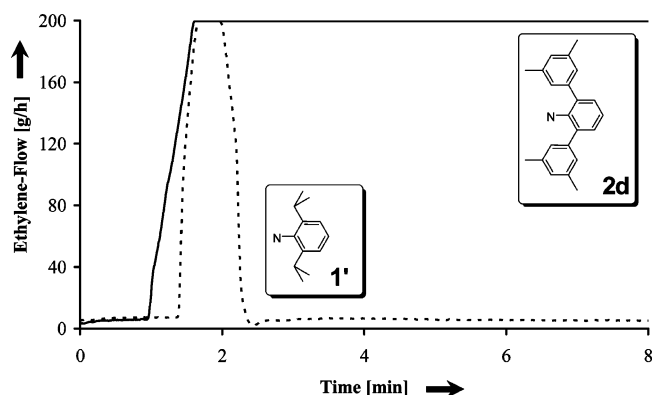
Figure 4. Ethylene flow diagrams of **1**′/TMA and **2d**/TMA of initial polymerization phase (2 data points/s).
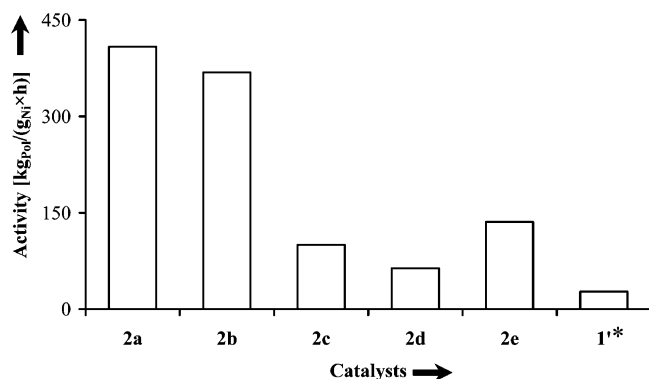
Figure 5. Polymerization activity at 60 °C at 10 bar monomer pressure and in the presence of hydrogen. (*) After 2.5 min no further activity.

Figure 6. Activity numbers at 80 °C and 10 or 30 bar monomer pressure in the presence of hydrogen. (*) Rapid and total deactivation of **1**′/TMA in the presence of hydrogen; no activity occurred at these conditions.

Figure 7. Molecular weight M_w development.

the primary CH signal at 38.10 ppm of the hexyl branching on the main chain, attributing these α, γ, β- signals to side chain carbons and not to end groups.

The growing amount of branches (methyl and longer) leads to a decline in melting temperature (110 to 90 °C, Table 3) and

crystallinity. Even changes in the physical material properties were observed (section 2.3). Since methyl branches can, to a

Table 3. Polymerization at 80 °C

no.	cat.[a]	P [bar]	X [n mmol H₂/ n mol C₂H₄]	yield [g]	activity [kg$_{Pol}$/(g$_{Ni}$ × h)]	M$_W$ × 10^{-5} [g/mol]	PDI	branches [‰]	T$_m$ [°C]
29	**1'**	10	0	14.75	25	3.5	2.6	93	*b*
30	**1'**	10	0.51	15.86	27	3.6	2.7	99	*b*
31	**1'**	30	0	6.39	11	4.9	2.4	80	40.7
32	**1'**	30	0.51	6.07	10	5.4	2.3	81	41.1
33	**2b**	10	3.84	32.26	165	1.4	2.1	12	118.4
34	**2b**	30	3.84	82.85	565	1.0	2.0	6	121.5
35	**2c**	10	3.84	13.3	23	2.0	2.3	30	92.2
36	**2c**	30	3.84	25.13	43	2.7	2.8	20	113.5
37	**2d**	5	1.92	13.75	23	0.6	1.7	43	85.1
38	**2d**	10	0	7.92	27	1.9	2.6	39	91.5
39	**2d**	10	0.51	12.90	44	1.9	2.2	37	91.0
40	**2d**	10	3.84	8.07	14	0.8	2.0	38	89.0
41	**2d**	30	0	27.65	47	4.9	2.2	30	102.5
42	**2d**	30	0.51	14.32	24	4.3	2.2	29	96.3
43	**2d**	30	1.92	13.14	22	1.3	2.0	21	101.7
44	**2d**	30	3.84	8.22	14	1.0	2.2	33	101.5
45	**2e**	10	0	3.1	5	3.4	2.4	48	75.5
46	**2e**	10	0.51	2.16	4	2.9	2.6	43	75.5
47	**2e**	10	1.92	4.58	8	2.7	1.9	46	76.5
48	**2e**	10	3.84	1.53	3	2.4	3.1	47	76.0
49	**2e**	30	0	7.11	12	4.4	1.9	36	89.6
50	**2e**	30	0.51	6.7	11	4.2	2.5	40	88.5
51	**2e**	30	3.84	9.8	17	1.6	1.9	34	92.6
52	**2a**	10	12.80	11.7	469	2.2	3.6	3	128.4

[a] 800 mL of toluene, 10 μmol of particular catalyst (in 4 mL of CH₂Cl₂); Al/Ni = 500, 1 h reaction time. [b] Amorphous material with no defined melting transition peak.
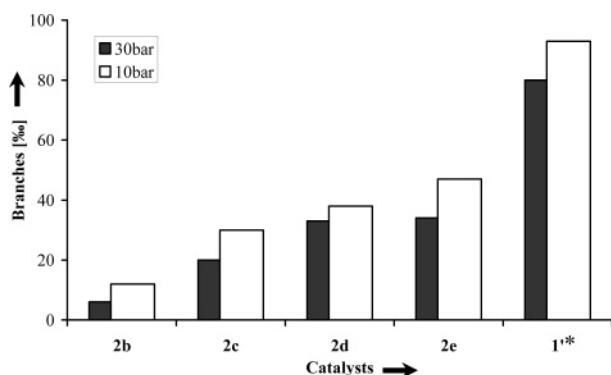

Figure 8. Microstructure control by tailor-made ligand design. (*) For comparison we include branching numbers in the polymer backbone produced in the absence of hydrogen.

Figure 9. Melting transition depends on branching numbers (regression of a linear equation: $R^2 = 0.94$).

certain extent, be incorporated into the PE crystal lattice,[30] we attribute this effect to the fraction of longer side groups. To our surprise, the highly substituted catalysts **2d,e**/TMA bearing eight substituents in 3,5-positions of the "*ortho*-aryl" rings lead to embranchments exceeding 30‰. The melting point declines in these materials down to values as low as 75 °C.[31]

The solid-state structure of **2f** (Figure 2) shows that a 4-*tert*-butyl-phenyl substitution on the aniline fragments forces the complex to adopt a rigid, C_2-symmetric coordination geometry. This offers enough space for ethylene coordination in front of the nickel(II) coordination plane, thus favoring chain propagation over the (space demanding) chain walking process. High activities in combination with ultrahigh molecular weights and narrow polydispersities are therefore characteristic for this complex type.[11] The 3,5-dimethyl substituted **2d** and especially **2e** bear
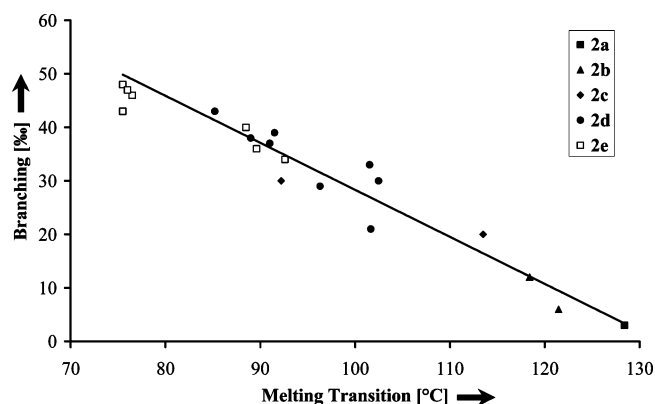
phenyl rings in the 2,6-position of the aniline fragments that are again in rigid face-to-face positions relative to each other, thus affording an almost ideal C_{2v}-symmetry in the solid state and most presumably also in solution. In contrast to **2g**, the 3,5-substitution of **2d′,e** offers much more space for ethylene coordination but also for chain end isomerization sequences ("chain walking") at the front side of the nickel(II) plane. In addition, ethylene attack and therefore chain transfer by associative olefin exchange from the apical positions are suppressed, so that branched polyethylenes of high molecular weights can be obtained at elevated temperatures. On the basis of the lead structure **2d**, control of the PE microstructure becomes possible through catalyst design by introduction of eight fluorine

(30) van der Ven, S. *Polypropylene and other Polyolefins*; Elsevier: Amsterdam, 1990; pp 468ff.

(31) In accord with theory, monomer pressure has a strong influence on the branching degree. However, experiments ran at 30 bar monomer pressure show the same trend **2b** ≈ **2c** < **2d** ≈ **2e** like that observed at 10 bar. Due to the outstanding activity performance of **2a**/TMA, we did not apply this catalyst system at 30 bar.
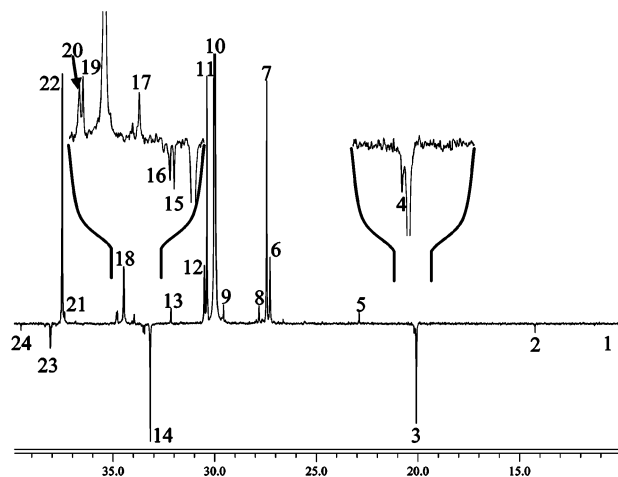
Figure 10. A typical DEPT spectrum of the polyethylene produced by **2d**/TMA (Table 3, entry 37). Labels are discussed in Table 4.

Table 4. Chemical Shifts δ and Their Assignment[a]

peak no.	DEPT	δ [ppm]	lit.[29,37,38]	monomer sequence	carbon
1	P	11.31	11.17	EBE	$1B_2$
2	P	14.23	14.13	ELE	$1B_{4-n}$
3	P	20.09	19.87	EPE	$1B_1$
4	P	20.19	20.57	EPP + PPE	$1B_1$
5	S	22.89	22.88	ELE	$2B_{5-n}$
6	S	27.29	27.28	BEE	βB_{6-n}
7	S	27.44	27.24	PEE + EEP	βB_1
8	S	27.83	27.97	PEP*	$1,6\text{-}\beta B_1$
9	S	29.57	29.58	ELE	$4B_{6-n}$
10	S	30.00	30.00	EEE	$\delta B_1, \delta B_{6-n}$
11	S	30.38	30.35	EEEP	γB_1
12	S	30.51	30.44	ELE + E^{i}BuE	γB_1
13	S	32.15	32.12	ELE	$3B_{6-n}$
14	T	33.18	33.10	EPE	brB_1
15	T	33.46	33.38	EP*PE + EP*PE (m)	$1,4\text{-}brB_1$
16	T	33.52	33.38	EP*PE + EP*PE (r)	$1,4\text{-}brB_1$
17	S	33.97	34.14	BEE	αB_2
18	S	34.49	34.40−34.94	ELE	$\alpha B_{(6-n)}$
19	S	34.79	34.22	EP*PE + EP*PE (m)	$1,4\text{-}\alpha B_1$
20	S	34.84	34.22	EP*PE + EP*PE (r)	$1,4\text{-}\alpha B_1$
21	S	37.40	37.45	EEPP + PPEE + EPEP	αB_1
22	S	37.50	37.45	EPE + EPEE	αB_1
23	T	38.10	38.00	ELE	brB_{6-n}
24	T	39.54	39.71	EBE	brB_2

[a] Label *x*B*y* in case *x* is a number: *x* gives the position of the carbon atom in a branch of length *y*. In case *x* is a Greek symbol: carbon in the main chain with 0, 1, 2, or 3 carbons from the branch, respectively, denoted as α, β, γ, and δ. Positive peaks in the DEPT experiment mean methylene groups (*S*econdary), negative methyl (*P*rimary), and methin groups (*Ter*tiary). In the fifth column unit sequences were used, where E is an ethylene unit (CH_2-CH_2), P is a propylene unit ($CH_2-CH(CH_3)$), P* is a 2,1 inserted propylene unit ((CH_3)CH$-CH_2$), L is a 1-alkene with a long branch ($CH_2-CH(CH_2)_{n\geq3}CH_3$). The exact unit carrying the carbon atom identified by the chemical shift indicated in the fifth column is underlined.

substituents (**2e**), four methyl groups (**2b**), or four trifluoromethyl groups (**2c**), respectively, influencing molecular weight, branching type, and distribution differently (Tables 2 and 3).

2a/TMA bears no substitution on the four 2,6-phenyl rings, thus showing a relatively open coordination environment around the Ni(II) atom. Interestingly, it produces with high activity exclusively linear polyethylene. In contrast to its bulky, higher

substituted analogues, we speculate here on the increased flexibility of the aniline fragments that might offer the chance of easy fluctuations around the N1−C6 bonds (Figure 1). We showed earlier by using 2-phenyl substituted complexes that there is no free rotation of 2-aryl substituted aniline moieties.[11] In the case of **2g**, this type of rapid torsional fluctuation again would reduce the front space necessary for chain walking, affording linear PE products. This hypothesis is supported by results published recently in an elegant work by Guan.[32] His group applied cyclophane-type, α-diimine nickel(II) catalysts structurally similar to **2g** but which froze such fluctuations by two 4,4′-ethyl bridges between adjacent aniline phenyl groups below and above the coordination plane, thus affording highly branched polyethylene again.

2.3. Mechanical Properties of Selected PE Samples. The influence of our aryl-substituted catalysts on macroscopic material properties through microstructural control was preliminarily investigated by using **2d** and **2b** (Chart 3), activated by TMA. Five PE samples of different molecular weights and branching content (Table 2, Table 3; entries 13, 33 and 22, 37, and 41) were tested by uniaxial stretching until failure. The degree of branching and consequently T_m vary in the range of 8−43‰ and 130−85 °C, respectively, with approximately equidistant branching differences between the investigated samples. The molecular weights are in the same order of magnitudes ($0.6 \times 10^5 \leq M_w \leq 4.9 \times 10^5$ g/mol).

The material densities are in the range of linear low-density PE (LLDPE, $d = 0.928$ g/cm^3) made classically in an ethylene copolymerization process with 1-butene with a particular branching concentration on the polymer chain of 24‰.[33] Using the differently substituted **2b,d**/TMA catalysts, even VLDPE (very low-density PE) (LLDPE, Table 5, $0.921 \leq d \leq 0.898$ g/cm^3) materials are accessible at elevated polymerization temperatures, which conventionally only result from metallocene catalyzed copolymerization reactions. The densities of all investigated samples are clearly below 0.961 g/cm^3 which is characteristic of HDPE grades bearing a concentration of short chain branches of 1.2‰.

Semicrystalline polymers, like the analyzed polyethylenes, exhibit both elastic (recoverable) and plastic (quasipermanent) deformation while exposed to external forces (Figure 11). Preliminary results show a characteristic steep increase of the stress at small elongations, determining Young's modulus of the material. The obtained deformation is mainly elastic and can be described by Hooke's law.[34] After this linear range the plastic flow in the sample sets is characterized by the yield point. The yield stress in the different polymers increases with their particular crystallinity, starting at about 4 MPa and ranging to 15 MPa. Excluding the sample with higher molecular weight (Table 5, entry 41), all polymers failed at $\lambda \approx 7$. The low crystalline specimens (Table 5, entries 22 and 37) showed no significant strain hardening compared to those with higher crystallinity (Table 5, entries 13 and 33). The existence of a strain hardening for one sample (Table 5, entry 41), characterized by the faster increase of the stress while stretching, can be attributed to its molecular weight which is higher compared to the other test specimen.[35]

(32) Camacho, D. H.; Salo, E. V.; Ziller, J. W.; Guan, Z. *Angew. Chem.* **2004**, *116*, 1857.
(33) Whiteley, K. S. In *Industrial Polymers Handbook: Products, Processes, Applications*; Wiley-VCH: Weinheim, 2001; Vol. 2, p 1205.
(34) Sperling, L. H. *Physical Polymer Science*; John Wiley & Sons: 1986.

Table 5. Exemplary Polyethylene Grades Chosen for Determination of the Physical Properties

no.[a]	cat.	density [g/cm³][36]	crystallinity from density [%]	crystallinity from DSC [%]	yield stress [MPa]	max elongation λ	max stress [Mpa]	T_m [°C]	branching [‰]
37	**2d**	0.898 45	33	35	4.0	7.0	12.5	85.2	43
41	**2d**	0.906 01	39	42	5.2	5.0	18.5	102.5	30
22	**2d**	0.914 02	45	48	9.1	7.4	14.0	110.1	23
33	**2b**	0.921 45	50	52	9.9	7.0	32.5	118.4	12
13	**2b**	0.928 48	55	66	15.5	7.4	37.2	130.7	8

[a] Polymerization results of entries 13 and 22 are tabulated in Table 2, and those of entries 33, 37, and 41, in Table 3.
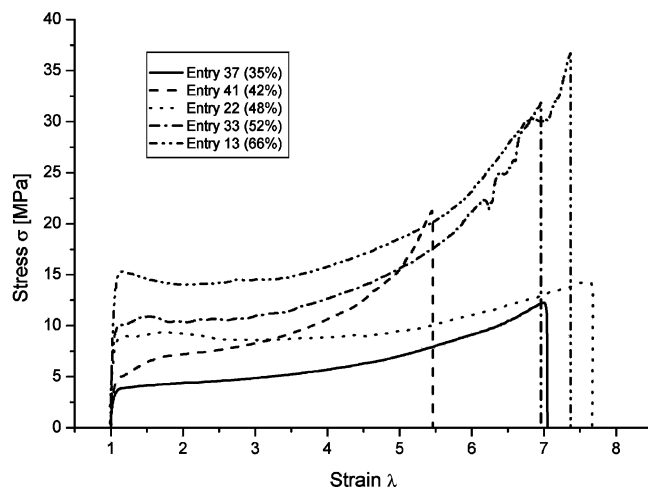

Figure 11. Exemplary stress−strain curves of representative polyethylenes. The strain is calculated via $\lambda = (l_a - l_i)/l_i$. l_a: Actual length of the sample. l_i: Initial length. The DSC crystallinity is given.

3. Conclusion

The development of early transition metal complexes as catalyst precursors for olefin polymerization marked a breakthrough in the history of metal-catalyzed insertion reactions. The pinpoint precise control of stereochemistry and therefore material rheology by the tailor-made complex architecture were important compound features for successful commercialization. However, the development of late transition metal, especially nickel, catalysts expand the portfolio of reaction sequences on the catalytically active center by the new chain end isomerization process ("chain walking"). These late-transition catalysts afford branched, high-value products exclusively from ethylene. Since then, however, commercial application of this initial invention remained cumbersome. One major reason is the rapid and quantitative deactivation reaction of **1** and **1′** in the presence of hydrogen that is inevitable as a chain transfer reagent.

The "*ortho*-aryl" substituted second generation complex family of the lead structure **2a** shows hydrogen stability. Additionally, the "*ortho*-aryl" groups of **2a** are prone to chemical modifications and are therefore ideal candidates for a tailor-made coordination geometry. The substituents of the particular complex determine the conelike space in front of the nickel center and thus define the chain propagation to chain end isomerization ratio. Complex design and X-ray diffraction analysis of new **2d′**, **e**, **f**, and **g** allowed us to predict the product microstructure. **2a**−**e** afford polymeric products, with a broad range of properties generated by the nature and concentration of branches, produced with high activity catalysts at elevated temperature and monomer pressure in the presence of hydrogen.

Future work will show if these new complexes can be supported and therefore made suitable for gas-phase polymerization processes. The novel material architectures that result from the most simple olefin, the ethylene monomer solely, will have to prove their applicability as commodity polymers or as specialized components in blend application.

Supporting Information Available: X-ray diffraction data were deposited at CCDC: deposition numbers are 644732 (**2d′**), 644731 (**2e**), 644729 (**2f**), and 644730 (**2g**). The Experimental Section as well as X-ray diffraction data of **2d′**, **e**, **f**, and **g** including tables of positional parameters for all atoms, anisotropic thermal parameters, all bond lengths and angles (CIF files) are available. This material is available free of charge via the Internet at http://pubs.acs.org.

JA070224I

(35) Jordens, K.; Wilkes, G. L.; Janzen, J.; Rohlfing, C. D.; Welch, M. B. *Polymer* **2000**, *41* (9), 7175.
(36) The used setup has an accuracy of $\pm 1.5 \times 10^{-6}$ g/cm³.
(37) Sahoo, S. K.; Zhang, T.; Reddy, D. V.; Rinaldi, P. L.; McIntosh, L. H.; Quirk, R. P. *Organometallics* **2003**, *36*, 4017.
(38) Usami, T.; Takayama, S. *Macromolecules* **1984**, *17*, 1756.